

Stabilizing Spin Coherence Through Environmental Entanglement in Strongly Dissipative Quantum Systems

Soumya Bera,¹ Serge Florens,¹ Harold U. Baranger,² Nicolas Roch,^{3,1} Ahsan Nazir,^{4,5} and Alex W. Chin⁶

¹*Institut Néel, CNRS and Université Grenoble Alpes, F-38042 Grenoble, France*

²*Department of Physics, Duke University, Durham, North Carolina 27708, USA*

³*Laboratoire Pierre Aigrain, École Normale Supérieure,*

CNRS (UMR 8551), Université Pierre et Marie Curie,

Université Denis Diderot, 24 rue Lhomond, 75231 Paris Cedex 05, France

⁴*Blackett Laboratory, Imperial College London, London SW7 2AZ, United Kingdom*

⁵*Photon Science Institute, The University of Manchester,*

Oxford Road, Manchester M13 9PL, United Kingdom

⁶*Theory of Condensed Matter Group, University of Cambridge,*

J J Thomson Avenue, Cambridge, CB3 0HE, United Kingdom

(Dated: July 31, 2018)

The key feature of a quantum spin coupled to a harmonic bath—a model dissipative quantum system—is competition between oscillator potential energy and spin tunneling rate. We show that these opposing tendencies cause environmental entanglement through superpositions of adiabatic and antiadiabatic oscillator states, which then stabilizes the spin coherence against strong dissipation. This insight motivates a fast-converging variational coherent-state expansion for the many-body ground state of the spin-boson model, which we substantiate via numerical quantum tomography.

The coupling of a quantum object to a macroscopic reservoir plays a fundamental role in understanding the complex transition from the quantum to the classical world. The study of such dissipative quantum phenomena has deep implications across a broad range of topics in physics [1], quantum technology [2], chemistry [3], and biology [4]. While quantum information stored in the quantum subsystem alone is lost during the interaction with the unobserved degrees of freedom in the reservoir, it is in principle preserved in the entangled many-body state of the global system. The nature of this complete wavefunction has received little attention, especially regarding the entanglement generated among the reservoir states. However, ultrafast experiments on solid-state and molecular nanostructures, including biological complexes, are increasingly able to probe the details of environmental degrees of freedom, whose quantum properties - particularly in non-perturbative regimes - may be key to understanding the device characteristics [5]. Our purpose here is to unveil a simple emerging structure of the wavefunctions in open quantum systems, using the complementary combination of numerical many-body quantum tomography and a systematic coherent-state expansion that efficiently encodes the entanglement structure of the bath. This combination of advanced techniques reveals how non-classical properties of the macroscopic environment can stabilise quantum coherence with respect to a purely semiclassical response of the bath.

An archetype for exploring the quantum dissipation problem [6–8] is to start with the simplest quantum object, a two-level system describing a generic quantum bit embodied by spin states $\{|\uparrow\rangle, |\downarrow\rangle\}$, and to couple it to an environment consisting of an infinite collection of

quantum oscillators a_k^\dagger (with continuous quantum number k and energy $\hbar\omega_k$). Quantum superposition of the two qubit states is achieved through a splitting Δ acting on the transverse spin component, while dissipation (energy exchange with the bosonic environment) and decoherence are provided by a longitudinal interaction term g_k with each displacement field in the bath. This leads to the Hamiltonian of the celebrated continuum spin-boson model (SBM) [6, 7]:

$$H = \frac{\Delta}{2} \sigma_x - \sigma_z \sum_k \frac{g_k}{2} (a_k^\dagger + a_k) + \sum_k \omega_k a_k^\dagger a_k, \quad (1)$$

where we set $\hbar = 1$, and the sums can be considered as integrals by introducing the spectral function of the environment, $J(\omega) \equiv \sum_k g_k^2 \delta(\omega - \omega_k)$. The generality of the SBM makes it a key model for studying non-equilibrium dynamics, non-Markovian quantum evolution, biological energy transport, and the preparation and control of exotic quantum states in a diverse array of systems [3, 6–9].

The possibility of maintaining robust spin superpositions in the ground and steady states of the SBM has attracted considerable attention, primarily due to its implications for quantum computing [10, 11]. Previous numerical approaches have focused on observables related to the qubit degrees of freedom [12–19], whilst a description of the global system-environment wavefunction has been confined to variational studies [20–24]. Variational theory readily predicts the formation of semiclassical polaron states, which involve the adiabatic response of the environmental modes to the spin tunneling, and thus the generation of strong entanglement between the qubit and the bath. However, we shall demonstrate here that the ground state of Hamiltonian (1) contains additional non-

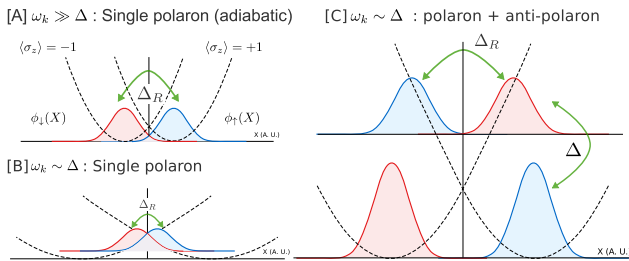


FIG. 1. (color online) Origins of polaron and antipolaron displacements in environmental wavefunctions. Black dashed lines are the spin-dependent potential energies of a single harmonic oscillator in the absence of spin tunneling ($\Delta = 0$), while blue (red) curves sketch the single-mode wavefunctions of the oscillator (in real space X) on the $\langle \sigma_z \rangle = 1$ (-1) potential surfaces. [A] High frequency modes ($\omega \gg \Delta$) tend to rest in the bottom of their (spin-dependent) potential due to the large energy of other displacements. This leads to the formation of adiabatic polarons. [B-C] Low frequency modes ($\omega \ll \Delta$) have shallow potentials with well-separated minima. The inter-minima wavefunction overlap is reduced while the potential cost of other displacements becomes less prohibitive. The oscillators can either climb up the potential landscape, gaining some tunneling energy (panel [B]), or become superposed with oppositely displaced states—“antipolarons”—so that tunneling and potential energy are both optimal (panel [C]). Superposition of such polaron and antipolaron states generates multimode entanglement in the complete environmental wavefunction.

classical correlations among the environmental oscillator modes arising from their *non*-adiabatic response to spin-flip processes. We find that this entanglement structure is key for the stabilization of qubit superpositions relative to the semiclassical picture, and, in addition, follows naturally from a systematic variational framework beyond the adiabatic polaron approximation.

In order to enlighten the nature of these emergent non-classical environmental states, we start by analyzing the SBM with qualitative arguments based on energetics. First, in the absence of tunneling, $\Delta = 0$, the ground state of H in Eq. (1) is doubly degenerate. In the corresponding wavefunctions, the oscillators displace classically, in a direction that is fully correlated with the spin projection (adiabatic response): $|\Psi_\uparrow\rangle = |\uparrow\rangle \otimes |+\!f^{\text{cl}}\rangle$ and $|\Psi_\downarrow\rangle = |\downarrow\rangle \otimes |-\!f^{\text{cl}}\rangle$. Here we introduce the product of semiclassical coherent states (displaced oscillators) $|\pm f\rangle \equiv e^{\pm \sum_k f_k (a_k^\dagger - a_k)} |0\rangle$, with the classical displacements $f_k^{\text{cl}} = \pm g_k/2\omega_k$ that shift each oscillator to the minimum of its static spin-dependent potential. This potential is evident in Eq. (1) for $\Delta = 0$ and is shown explicitly in Fig. 1A.

For $\Delta \neq 0$, the oscillators experience a competition between spin tunneling and oscillator displacement energy. For high frequency modes ($\omega_k \gg \Delta$), transitions to other oscillator states are suppressed by the steep curvature of the potential (Fig. 1A). Thus, these oscillators adi-

abatically tunnel with the spin between potential minima; the displacement of the oscillators reduces their overlap, suppressing the tunneling amplitude to a value $\Delta_R \ll \Delta$. Extending this argument to low frequency modes ($\omega_k \ll \Delta$) reveals a problem: the large separation of the minima ($g_k/2\omega_k$) causes poor wavefunction overlap that prevents tunneling of the spin, thus destroying spin superposition. The classic scenario to overcome this problem is to adjust the displacements to smaller values, sacrificing potential energy to maintain spin-tunneling energy through better overlap (Fig. 1B). Here, we argue for a new alternative scenario: because the potential surface is shallow for low frequency modes, transitions to other oscillator states become possible. Indeed, it is favorable for the oscillator wavefunction to include superpositions of coherent states with displacements *opposite* to those dictated by the spin. In that way, direct tunneling transitions between the two potential surfaces are favored whilst keeping the main weight of the wavefunctions at low energy. We call these oppositely displaced oscillators “antipolaron” states.

The strong competition between spin tunneling and oscillator displacement cannot indeed be fulfilled by a single coherent state, even if optimized variationally. The latter has been pursued in numerous variational studies [20–24], embodied by the so-called Silbey-Harris (SH) Ansatz for the ground state of the spin-boson model [20, 21]:

$$|\Psi^{\text{SH}}\rangle = |\uparrow\rangle \otimes |+\!f^{\text{SH}}\rangle - |\downarrow\rangle \otimes |-\!f^{\text{SH}}\rangle, \quad (2)$$

where the displacements $f_k^{\text{SH}} = [g_k/2]/(\omega_k + \Delta_R)$ are determined by the variational principle. (Note that this Ansatz respects the symmetries of the Hamiltonian in the absence of a magnetic field along \hat{z} .) While this simple state possesses virtues, such as an accurate estimate of the renormalized tunneling frequency $\Delta_R = \Delta e^{-2 \sum_k (f_k^{\text{SH}})^2}$, it also has severe defects, such as spurious transitions [23, 25–28] and a drastic underestimation of the qubit coherence $\langle \sigma_x \rangle$. Further works aiming at refining the variational Ansatz focused on the simple single-mode case [29–31], or were restricted to a non fully-optimal variational state [32]. In light of the above discussion, the defects of the SH Ansatz are readily traced back to the lack of bath entanglement in wavefunction (2)—only the polaronic response is encoded in f_k^{SH} . To capture the missing antipolaronic contributions and so the complete entanglement structure of the bath, we propose here a systematic coherent-state expansion of the many-body ground state:

$$|\Psi\rangle = \sum_{n=1}^N C_n \left[|\uparrow\rangle \otimes |+\!f^{(n)}\rangle - |\downarrow\rangle \otimes |-\!f^{(n)}\rangle \right], \quad (3)$$

with $|\pm f^{(n)}\rangle = e^{\pm \sum_k f_k^{(n)} (a_k^\dagger - a_k)} |0\rangle$ the n^{th} coherent state appearing in the wavefunction. As is well known in many-body and chemical physics, variational methods

may be greatly improved w.r.t. convergence by optimized basis choices. For the spin boson model, coherent states are naturally selected, as was understood from the $\Delta = 0$ limit, and are in addition very simple to parametrize in terms of displacements. As we will see, the coherent state expansion allows convergence to be achieved with far fewer variational parameters than a brute-force variation of the (exponentially large) coefficients of a full configuration (Fock) basis of the environment states. This is due to the energetic constraints discussed above, which strongly reduce the phase space volume of the allowed displacements $f_k^{(n)}$. Indeed, for $\omega_k > \Delta_R$, each displacement function $f_k^{(n)}$ (for fixed n) will undergo quantum fluctuations between the polaronic and antipolaronic branches, $f_k^{\text{pol.}} \simeq g_k/(2\omega_k)$ and $f_k^{\text{anti.}} \simeq -g_k/(2\omega_k)$, respectively. The main freedom in fixing a given displacement $f_k^{(n)}$ is then in determining the crossover frequency from polaron to antipolaron behavior. As a consequence (see below), physical properties are very precisely determined for moderate values of N , the number of coherent states involved in wavefunction (3).

We can now readily understand how the emergence of environmental entanglement preserves spin coherence at strong dissipation. In the single-polaron Silbey-Harris theory, the spin coherence $\langle \sigma_x \rangle \simeq e^{-2 \sum_k (f_k^{\text{SH}})^2} = \Delta_R/\Delta$ is incorrectly controlled by the exponentially small renormalized tunneling frequency Δ_R . In contrast, the general wavefunction (3) contains additional contributions to $\langle \sigma_x \rangle$ of the type $e^{-\frac{1}{2} \sum_k (f_k^{(n)} + f_k^{(m)})^2}$ for $n \neq m$. Quantum fluctuations that favor antipolarons will flip the sign of one displacement with respect to the other, reducing the value of the sum, and drastically increasing the exponential with respect to the strongly suppressed value Δ_R/Δ . Thus, environmental correlations built into a multi-mode Schrödinger cat state affect the qubit properties in a dramatic way.

We now turn to calculating the wavefunction Eq. (3), where the displacements $f_k^{(n)}$ and coefficients C_n are determined by minimizing the total ground state energy $E = \langle \Psi | H | \Psi \rangle / \langle \Psi | \Psi \rangle$ for a fixed number N of coherent states ($1 \leq n \leq N$) [33]. We focus here on the standard case of Ohmic dissipation [6, 7], although our results should apply similarly to any type of spectral density. The continuous bath of bosonic excitations then assumes a linear spectrum in frequency, $J(\omega) \equiv \sum_k g_k^2 \delta(\omega - \omega_k) = 2\alpha\omega\theta(\omega_c - \omega)$, up to a high frequency cutoff ω_c , while the dissipation strength is given by the dimensionless parameter α . As a key check on the variational solution, we carry out an exact non-perturbative solution of the SBM using the numerical renormalization group (NRG) [34]; for example, the spin coherence $\langle \sigma_x \rangle$, to which we shall compare the variational result, is shown in Fig. 2.

The variational principle leads to a set of displacements $f_k^{(n)}$, shown in Fig. 2, that corroborate the physical picture given above: in addition to a fully positive displace-

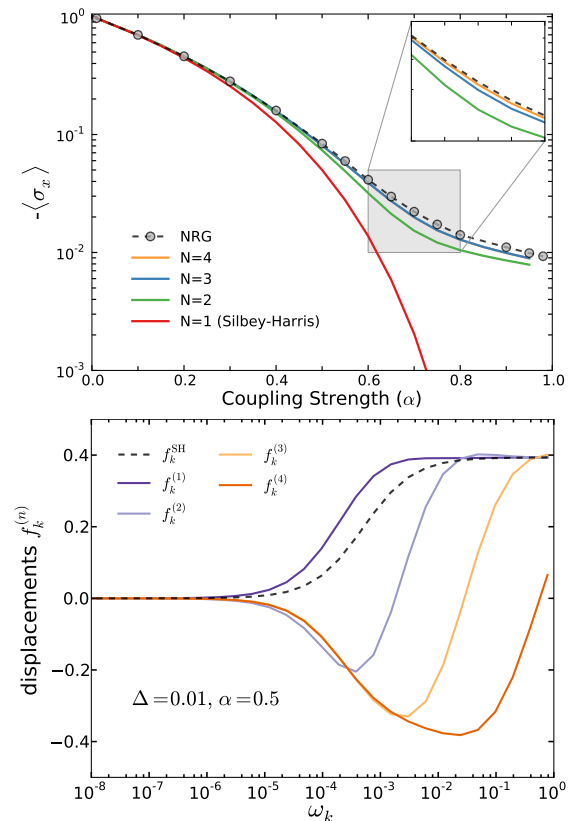


FIG. 2. Upper panel: Ground state coherence $-\langle \sigma_x \rangle$ as a function of dissipation strength α computed with the NRG (circles) for $\Delta/\omega_c = 0.01$ and compared to the results of the expansion Eq. (3) with $N = 1, 2, 3, 4$ coherent states. The inclusion of an antipolaronic component to the wavefunction ($N \geq 2$) has a drastic effect on the spin coherence. Lower panel: Displacements determined at order $N = 1$ (dashed line) and $N = 4$ (solid lines), showing the emergence of three antipolaron states at low energies, which merge smoothly onto the polaron state at high energy (adiabatic regime) [35]. Parameters are $\alpha = 0.5$ and $\Delta/\omega_c = 0.01$.

ment function $f_k^{(1)}$ (akin to the Silbey-Harris f_k^{SH} albeit quantitatively different), we find that all the other displacements undergo a crossover from positive value at high frequency to negative at low frequency. The total wavefunction (3) is thus strongly entangled.

This environmental entanglement drastically affects the spin coherence $\langle \sigma_x \rangle$: note the difference in Fig. 2 between the $N = 2$ and $N = 1$ solutions. In the latter, the coherence is given by the tiny renormalized qubit frequency, $\Delta_R = \Delta(\Delta e/\omega_c)^{\alpha/(1-\alpha)}$ for $\Delta/\omega_c \ll 1$. As the number of polarons increases, however, the variational solution rapidly converges to the exact NRG result, even capturing the saturation at strong dissipation $-\langle \sigma_x \rangle = \Delta/\omega_c$ for $\alpha \rightarrow 1$ [36]. These panels thus confirm one important message of our study: emergent entanglement within the environment stabilizes coherence of the spin, a result that is robust with respect to coupling the

whole system to a low temperature thermal bath [33].

We finally provide firm support for the above scenario by developing a many-body quantum tomography technique that allows direct characterization of the ground-state wavefunction based on non-perturbative NRG computations. While one cannot plot the complete many-body wavefunction, aspects can be accessed via standard Wigner tomography [1, 37] a technique which has witnessed impressive experimental developments lately in the field of superconducting circuits [38–40]. We choose to trace out all modes except the qubit degree of freedom together with a single bath mode with quantum number k . Projecting first onto only the $|\uparrow\rangle$ part of the wavefunction, we obtain the Wigner function $W_{\uparrow\uparrow}^{(k)}(X)$ as a function of the displacement X of oscillator k . For the wavefunction (3), this has a straightforward interpretation [1, 33]: the probability in phase space is simply the sum of Gaussian peaks centered at $X \simeq (f_k^{(n)} + f_k^{(m)})/2$. For high energy modes (adiabatic regime), all displacements are polaronic, $f_k^{(n)} \simeq f_k^{\text{cl}} = g_k/(2\omega_k)$, so that a single shifted Gaussian appears in $W_{\uparrow\uparrow}^{(k)}(X)$, see Fig. 3(a). A single coherent state [*i.e.* the Ansatz (2)] is sufficient in this high frequency regime to reproduce the NRG data perfectly, demonstrating the presence of polarons in the wavefunction.

Antipolarons appear more clearly in the spin off-diagonal ground state Wigner function $W_{\uparrow\downarrow}^{(k)}(X)$, rather than in $W_{\uparrow\uparrow}^{(k)}(X)$. Note that such conditional Wigner tomography was considered for instance in recent measurements of the moments $\langle\langle (a^\dagger)^n (a)^m \sigma^i \rangle\rangle$ for a carefully prepared state entangling microwave photons and a superconducting qubit in a circuit QED experiment [40]. In $W_{\uparrow\uparrow}^{(k)}(X)$, the antipolarons are hidden because their weights C_n tend to be smaller than that of the main polaron. In contrast, $W_{\uparrow\downarrow}^{(k)}(X)$ is governed by cross polaron-antipolaron contributions which peak at $X \simeq \pm(f_k^{(n)} - f_k^{(m)})/2$ [33]; other terms of polaron-polaron type have an exponentially small weight of order Δ_R . The emergence of antipolaronic, namely opposite, displacements in $f^{(n)}$ and $f^{(m)}$ should thus appear as a pair of symmetric Gaussians in $W_{\uparrow\downarrow}^{(k)}(X)$. This is indeed observed in the NRG data for intermediate frequencies, when adiabatic and antiadiabatic entanglement is maximal, as shown in Fig. 3(b). In this case, a single coherent state (fully polaronic) completely fails, but our expansion (3) quickly converges to the NRG results.

In conclusion, we have shown how environmental entanglement emerges in the ground state wavefunction of the spin-boson model, and why it surprisingly has a dramatic influence on the qubit coherence. This understanding led us to develop a general framework to rationalize many-body wavefunctions in strongly interacting open quantum systems. Proposals have been made to realize the strongly dissipative spin-boson model in

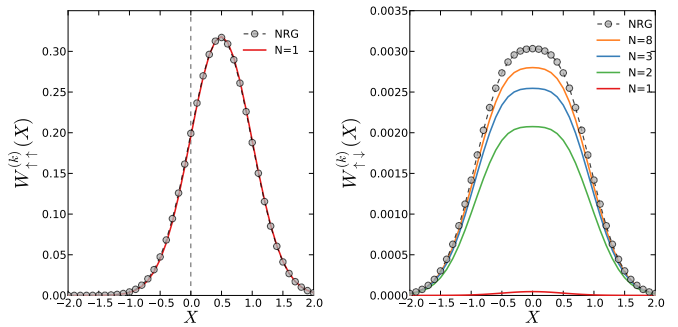


FIG. 3. Left: Spin-diagonal Wigner distribution, as obtained from the NRG, computed for a high energy mode. Polaron formation leads to a classical shift $X = f_k^{\text{cl}}$, that is fully captured by the Silbey-Harris state (single coherent state). Right: The spin-off-diagonal Wigner function is badly approximated by the single polaron $N = 1$ state, as antipolaron contributions dominate in this quantity. A single antipolaron ($N = 2$) quickly restores the correct magnitude, and reveals a pair of shifted Gaussians, as expected (see text). [Parameters here are $\alpha = 0.8$ and $\Delta/\omega_c = 0.01$.]

various physical systems [42, 43], most notably by coupling a superconducting qubit to Josephson junction arrays [41, 44], giving hope that experimental studies of environmental states should become accessible in the near future. The advances made in the present work opens the door to a better understanding of several interesting issues, such as photon transport in dissipative models [41, 44], quantum phase transitions for sub-Ohmic baths [16, 34], and studies of biased spin-boson systems [23].

S.B., S.F., and H.U.B. thank the Grenoble Nanoscience Foundation for funding under RTRA contract CORTRANO, and support by US DOE, Division of Materials Sciences and Engineering, under Grant No. desc0005237. A.N. thanks Imperial College and the University of Manchester for support. A.W.C. acknowledges support from the Winton Programme for the Physics of Sustainability.

-
- [1] J. M. Raimond and S. Haroche, *Exploring the Quantum* (Oxford Graduate Series, 2006).
 - [2] A. M. Nielsen and I. L. Chuang, *Quantum Computation and Quantum Information* (Cambridge University Press, New York, 2007).
 - [3] A. Nitzan, *Chemical Dynamics in Condensed Phases: Relaxation, Transfer and Reactions in Condensed Molecular Systems* (Oxford University Press, 2006).
 - [4] N. Lambert, Y.-N. Chen, Y.-C. Cheng, C.-J. Li, G.-Y. Chen, and F. Nori, *Nature Phys.* **9**, 10 (2013).
 - [5] A. W. Chin, J. Prior, R. Rosenbach, F. Caycedo-Soler, S. F. Huelga, and M. B. Plenio, *Nature Phys.* **9**, 113 (2013).
 - [6] A. J. Leggett, S. Chakravarty, A. T. Dorsey, M. P. A. Fisher, A. Garg, and W. Zwerger, *Rev. Mod. Phys.* **59**, 1

- (1987).
- [7] U. Weiss, *Quantum Dissipative Systems* (World Scientific, 1993).
- [8] H.-P. Breuer and F. Petruccione, *The Theory of Open Quantum Systems*, (Oxford University Press, 2010).
- [9] G. Scholes, G. Fleming, A. Olaya-Castro, and R. van Grondelle, *Nature Chem.* **3**, 763 (2011).
- [10] D. Jennings, A. Dragan, S. D. Barrett, S. D. Bartlett, and T. Rudolph, *Phys. Rev. A* **80**, 032328 (2009).
- [11] R. Raussendorf and H. J. Briegel, *Phys. Rev. Lett.* **86**, 5188 (2001).
- [12] R. Bulla, T. A. Costi, and T. Pruschke, *Rev. Mod. Phys.* **80**, 395 (2008).
- [13] N. Makri, *J. Math. Phys.* **36**, 2430 (1995).
- [14] H. Wang and M. Thoss, *New J. Phys.* **10**, 115005 (2008).
- [15] P. Nalbach and M. Thorwart, *Phys. Rev. B* **81**, 054308 (2010).
- [16] A. Winter, H. Rieger, M. Vojta, and R. Bulla, *Phys. Rev. Lett.* **102**, 030601 (2009).
- [17] A. Alvermann and H. Fehske, *Phys. Rev. Lett.* **102**, 150601 (2009).
- [18] J. Prior, A. W. Chin, S. F. Huelga, and M. B. Plenio, *Phys. Rev. Lett.* **105**, 050404 (2010).
- [19] S. Florens, A. Freyn, D. Venturelli, and R. Narayanan, *Phys. Rev. B* **84**, 155110 (2011).
- [20] V. J. Emery and A. Luther, *Phys. Rev. Lett.* **26**, 1547 (1971).
- [21] R. Silbey and R. A. Harris, *J. Chem. Phys.* **80**, 2615 (1984); R. A. Harris and R. Silbey, *J. Chem. Phys.* **83**, 1069 (1985).
- [22] A. W. Chin, J. Prior, S. F. Huelga, and M. B. Plenio, *Phys. Rev. Lett.* **107**, 160601 (2011).
- [23] A. Nazir, D. P. S. McCutcheon, and A. W. Chin, *Phys. Rev. B* **85**, 224301 (2012).
- [24] K. Agarwal, I. Martin, M. D. Lukin, and E. Demler, *Phys. Rev. B* **87**, 144201 (2013).
- [25] D. P. S. McCutcheon and A. Nazir, *J. Chem. Phys.* **135**, 114501 (2011).
- [26] C. K. Lee, J. Moix, and J. Cao, *J. Chem. Phys.* **136**, 204120 (2012).
- [27] A. Chin and M. Turlakov, *Phys. Rev. B* **73**, 075311 (2006).
- [28] Z.-D. Chen and H. Wong, *Phys. Rev. B* **78**, 064308 (2008).
- [29] J. Stolze and L. Müller, *Phys. Rev. B* **42**, 6704 (1990).
- [30] Q.-B. Ren and Q.-H. Chen, *Chin. Phys. Lett.* **22**, 2914 (2005).
- [31] M.-J. Hwang and M.-S. Choi, *Phys. Rev. A* **82**, 025802 (2010).
- [32] H. Zheng and Z. Lü, *J. Chem. Phys.* **138**, 174117 (2013).
- [33] Please see the Supplementary Information for details.
- [34] R. Bulla, N.-H. Tong, and M. Vojta, *Phys. Rev. Lett.* **91**, 170601 (2003).
- [35] In the NRG logarithmic discretisation of the bath spectrum, frequency points are unevenly spaced, leading to a saturation of f_k at high frequencies, instead of the fall off obtained for a linear energy mesh.
- [36] K. Le Hur, *Ann. Phys.* **323**, 2208 (2008).
- [37] A. I. Lvovsky and M. G. Raymer, *Rev. Mod. Phys.* **81**, 299 (2009).
- [38] M. Hofheinz, H. Wang, M. Ansmann, R. C. Bialczak, E. Lucero, M. Neeley, A. D. O'Connell, D. Sank, J. Wenner, J. M. Martinis, and A. N. Cleland, *Nature* **459**, 546 (2009).
- [39] C. Eichler, D. Bozyigit, C. Lang, L. Steffen, J. Fink, and A. Wallraff, *Phys. Rev. Lett.* **106**, 220503 (2011).
- [40] C. Eichler, C. Lang, J. M. Fink, J. Govenius, S. Filipp, and A. Wallraff, *Phys. Rev. Lett.* **109**, 240501 (2012).
- [41] K. Le Hur, *Phys. Rev. B* **85**, 140506 (2012).
- [42] A. Recati, P. O. Fedichev, W. Zwerger, J. von Delft, and P. Zoller, *Phys. Rev. Lett.* **94**, 040404 (2005).
- [43] D. Porras, F. Marquardt, J. von Delft, and J. I. Cirac, *Phys. Rev. A* **78**, 010101(R) (2008).
- [44] M. Goldstein, M. H. Devoret, M. Houzet, and L. I. Glazman, *Phys. Rev. Lett.* **110**, 017002 (2013).

Supplementary information for ‘‘Stabilizing spin coherence through environmental entanglement in strongly dissipative quantum systems’’

We present here basic technical details on the different methods used in the main text. In the first part, we derive from the coherent state expansion various physical quantities of interest: ground state energy, spin coherence and single-mode Wigner functions. In the second part, we provide information on how the (standard) numerical renormalization group simulations were set up in order to perform the Wigner tomography. Finally, the third part presents finite temperature calculations, which indicate that the emergence of antipolarons is robust to thermal effects.

GENERAL COHERENT STATE EXPANSION IN OPEN QUANTUM SYSTEMS

Energetics of the trial state

We consider the unbiased spin-boson model, [1, 2] as defined by the Hamiltonian (1) of the main text:

$$H = \frac{\Delta}{2}\sigma_x + \sum_k \omega_k a_k^\dagger a_k - \sigma_z \sum_k \frac{g_k}{2}(a_k^\dagger + a_k), \quad (\text{S1})$$

with tunneling energy Δ , a set of oscillator frequencies ω_k , and system-oscillator coupling strengths g_k (assumed real). Here, $\sigma_z = |\uparrow\rangle\langle\uparrow| - |\downarrow\rangle\langle\downarrow|$, with spin basis states $|\downarrow\rangle$ and $|\uparrow\rangle$, and a_k^\dagger (a_k) is the oscillator creation (annihilation) operator for mode k . Hamiltonian (S1) spans the cases of few discrete modes up to a continuum of bosonic fields, in which case the discrete k -sum ought to be replaced by an integral over energy.

The ground state wavefunction is expanded on an infinite set of coherent states, as discussed in the main text:

$$|\Psi\rangle = \sum_{n=1}^{\infty} C_n \left[|\uparrow\rangle \otimes |+f^{(n)}\rangle - |\downarrow\rangle \otimes |-f^{(n)}\rangle \right], \quad (\text{S2})$$

where the bosonic part of the wavefunction involves coherent states of the form

$$|\pm f^{(n)}\rangle = e^{\pm \sum_k f_k^{(n)}(a_k^\dagger - a_k)} |0\rangle, \quad (\text{S3})$$

defined as products of displaced states, where $|0\rangle$ represents all oscillators being in the vacuum state. The presence of a \mathbb{Z}_2 symmetry, namely ($|\uparrow\rangle \rightarrow |\downarrow\rangle$, $|\downarrow\rangle \rightarrow |\uparrow\rangle$, $a_k \rightarrow -a_k$), and the need for minimizing the spin tunneling energy enforces the chosen relative sign between the up and down components of the ground state wavefunction in Eq. (S2).

Displacements $f_k^{(n)}$ and weights C_n are taken as free parameters (both are real numbers), that will be varied to minimise the total ground state energy $E = \langle\Psi|H|\Psi\rangle/\langle\Psi|\Psi\rangle$, with

$$\langle\Psi|H|\Psi\rangle = -\Delta \sum_{n,m} C_n C_m e^{-\frac{1}{2} \sum_q [f_q^{(n)} + f_q^{(m)}]^2} + \sum_{n,m} C_n C_m \sum_k 2\omega_k f_k^{(n)} f_k^{(m)} e^{-\frac{1}{2} \sum_q [f_q^{(n)} - f_q^{(m)}]^2} \quad (\text{S4})$$

$$- \sum_{n,m} C_n C_m \sum_k g_k [f_k^{(n)} + f_k^{(m)}] e^{-\frac{1}{2} \sum_q [f_q^{(n)} - f_q^{(m)}]^2} \quad (\text{S5})$$

and $\langle\Psi|\Psi\rangle = 2 \sum_{n,m} C_n C_m e^{-\frac{1}{2} \sum_q [f_q^{(n)} - f_q^{(m)}]^2}$.

In the case of a single coherent state, we recover the usual Silbey-Harris energy functional: [3]

$$E^{(\text{SH})} = -\frac{\Delta}{2} e^{-2 \sum_k (f_k^{(\text{SH})})^2} + \sum_k \omega_k (f_k^{(\text{SH})})^2 - \sum_k g_k f_k^{(\text{SH})}, \quad (\text{S6})$$

with the displacement $f_k^{(\text{SH})} = [g_k/2]/(\omega_k + \Delta_R)$ readily obtained from the variational principle, $\partial E^{(\text{SH})}/\partial f_k^{(\text{SH})} = 0$.

Ground state spin coherence

The coherent-state expansion (S2) for the wavefunction allows us to compute in a simple way all physical observables. We start with the spin coherence in the ground state, a quantity that was discussed in detail in the main text. We readily find:

$$\langle \sigma_x \rangle = -\frac{\sum_{n,m} C_n C_m e^{-\frac{1}{2} \sum_q [f_q^{(n)} + f_q^{(m)}]^2}}{2 \sum_{n,m} C_n C_m e^{-\frac{1}{2} \sum_q [f_q^{(n)} - f_q^{(m)}]^2}}. \quad (\text{S7})$$

This expression was used to determine the spin coherence in Fig. 2A of the main text.

Spin-diagonal single-mode Wigner function

We discuss here the spin-dependent Wigner distributions associated to the reduced density matrix defined in the subspace spanned by the qubit and one *given* oscillator mode with frequency ω_k . The qubit degrees of freedom can be used for filtering out the polaron and antipolaron contributions within the wavefunction, thanks to appropriate insertions of Pauli matrices in the standard definition of the Wigner function. [4] We consider here the projection onto the $|\uparrow\rangle$ component only:

$$W_{\uparrow\uparrow}^{(k)}(X) = \frac{1}{\langle \Psi | \Psi \rangle} \int \frac{d^2\lambda}{\pi^2} e^{X(\bar{\lambda}-\lambda)} \langle \Psi | e^{\lambda a_k^\dagger - \bar{\lambda} a_k} \frac{1 + \sigma_z}{2} | \Psi \rangle. \quad (\text{S8})$$

This Wigner distribution can be evaluated using the coherent state expansion of the ground state (S2).

$$W_{\uparrow\uparrow}^{(k)}(X) = \frac{1}{\langle \Psi | \Psi \rangle} \int \frac{d^2\lambda}{\pi^2} e^{X(\bar{\lambda}-\lambda)} \sum_{n,m} C_n C_m \langle f^{(n)} | e^{\lambda a_k^\dagger - \bar{\lambda} a_k} | f^{(m)} \rangle. \quad (\text{S9})$$

Using standard coherent state algebra, we easily obtain the required overlaps,

$$\langle f^{(n)} | e^{\lambda a_k^\dagger - \bar{\lambda} a_k} | f^{(n)} \rangle = e^{(\lambda - \bar{\lambda}) f_k^{(n)}} e^{-\lambda \bar{\lambda} / 2} \quad (\text{S10})$$

$$\langle f^{(n)} | e^{\lambda a_k^\dagger - \bar{\lambda} a_k} | f^{(m)} \rangle = e^{-\frac{1}{2} \sum_q (f_q^{(n)} - f_q^{(m)})^2} e^{\lambda f_k^{(n)} - \bar{\lambda} f_k^{(m)}} e^{-\lambda \bar{\lambda} / 2} \quad (\text{S11})$$

$$\langle f^{(m)} | e^{\lambda a_k^\dagger - \bar{\lambda} a_k} | f^{(m)} \rangle = e^{(\lambda - \bar{\lambda}) f_k^{(m)}} e^{-\lambda \bar{\lambda} / 2}. \quad (\text{S12})$$

Performing the Gaussian integral in Eq. (S9) yields:

$$W_{\uparrow\uparrow}^{(k)}(X) = \frac{1}{\pi \langle \Psi | \Psi \rangle} \sum_{n,m} C_n C_m e^{-\frac{1}{2} \sum_{q \neq k} (f_q^{(n)} - f_q^{(m)})^2} e^{-2 \left(X - \frac{f_k^{(n)} + f_k^{(m)}}{2} \right)^2}. \quad (\text{S13})$$

In the adiabatic limit $\omega_k \gg \Delta$, all displacements become classical, $f_k^{(n)} \simeq f_k^{\text{cl}} = g_k / (2\omega_k)$, so that the Wigner function reduces to a single Gaussian centered on $X \simeq g_k / (2\omega_k)$, as demonstrated in Fig. 3A of the main text.

Spin-off-diagonal single-mode Wigner function

In order to highlight the emergence of antipolaronic contributions in the wavefunction, we now insert the off-diagonal σ_x Pauli matrix in the usual definition of the Wigner function:

$$W_{\uparrow\downarrow}^{(k)}(X) = \frac{1}{\langle \Psi | \Psi \rangle} \int \frac{d^2\lambda}{\pi^2} e^{X(\bar{\lambda}-\lambda)} \langle \Psi | e^{\lambda a_k^\dagger - \bar{\lambda} a_k} \sigma_x | \Psi \rangle. \quad (\text{S14})$$

From the trial state (S2), we get:

$$W_{\uparrow\downarrow}^{(k)}(X) = \frac{1}{\langle \Psi | \Psi \rangle} \int \frac{d^2\lambda}{\pi^2} e^{X(\bar{\lambda}-\lambda)} \sum_{n,m} C_n C_m \langle -f^{(n)} | e^{\lambda a_k^\dagger - \bar{\lambda} a_k} | f^{(m)} \rangle. \quad (\text{S15})$$

A computation similar to the one performed above leads to the final result:

$$W_{\uparrow\downarrow}^{(k)}(X) = \frac{1}{\pi \langle \Psi | \Psi \rangle} \sum_{n,m} C_n C_m e^{-\frac{1}{2} \sum_{q \neq k} (f_q^{(n)} + f_q^{(m)})^2} \left[e^{-2 \left(X - \frac{f_k^{(n)} - f_k^{(m)}}{2} \right)^2} + e^{-2 \left(X + \frac{f_k^{(n)} - f_k^{(m)}}{2} \right)^2} \right]. \quad (\text{S16})$$

The above expression shows important differences from the $|\uparrow\rangle$ -projected Wigner distribution of Eq. (S13). First, Gaussian peaks form at position near the difference of two displacements, $X \simeq \frac{f_k^{(n)} - f_k^{(m)}}{2}$, so that the formation of antipolarons results in finite displacements. Second, the main polaron contribution, $n = m = 1$, is suppressed by the tiny factor $e^{-2 \sum_{q \neq k} (f_q^{(1)})^2} \simeq \Delta_R / \Delta \ll 1$, in contrast to the spin-diagonal Wigner function (S13), where it appears with a prefactor of order one. Antipolarons are thus best resolved in the spin-off-diagonal Wigner function (S16), as checked in Fig. 3B of the main text.

IMPLEMENTATION OF THE NRG CALCULATIONS

The numerical solution of the spin-boson Hamiltonian (S1) with continuous spectrum relies on a logarithmic shell blocking of the bosonic modes onto energy intervals $[\Lambda^{-n-1}\omega_c, \Lambda^{-n}\omega_c]$ (with $\Lambda = 2$ in all our calculations). This defines Wilson-shell bosonic creation operators:

$$a_n^\dagger = \int_{\Lambda^{-n-1}\omega_c}^{\Lambda^{-n}\omega_c} dk a_k^\dagger. \quad (\text{S17})$$

The resulting discrete Hamiltonian, which spans from arbitrarily small energy up to the high energy cutoff ω_c , is then iteratively diagonalised according to the Numerical Renormalization Group (NRG) algorithm [5, 6]. One novel part of the NRG simulations performed for this work lies in the computation of the Wigner distribution reduced to the joint spin and single k -mode subspace. In order to implement Eqs. (S8) and (S14), we first define arbitrary moments of the chosen oscillator with frequency $\omega_k = \omega_c \Lambda^{-n}$:

$$A_{\sigma_i; m, m'}^{(k)} = \langle \Psi | \sigma_i [a_n^\dagger]^m [a_n]^{m'} | \Psi \rangle, \quad (\text{S18})$$

with $i = 0, x, y, z$ labelling the Pauli matrices related to the spin projection (we take $\sigma_0 \equiv 1$) and m, m' positive integers. Such ground state observables are readily computed within the NRG algorithm (for typically $0 \leq m, m' < 10$). One can then expand Eqs. (S8) and (S14) in a power series in λ and $\bar{\lambda}$, yielding

$$W_{\sigma_i}^{(k)}(X) = \frac{2}{\pi} \sum_{m, m'=0}^{+\infty} A_{\sigma_i; m, m'}^{(k)} \frac{(-1)^{m+m'}}{m! m'!} \frac{\partial^{m+m'}}{\partial X^{m+m'}} e^{-2X^2}. \quad (\text{S19})$$

The wanted Wigner distributions are now solely expressed in terms of the NRG-computable moments $A_{\sigma_i; m, m'}^{(k)}$, and are shown in Fig. 3 of the main text.

FINITE TEMPERATURE EFFECTS

One striking feature of the many-body ground state of the spin-boson model is that the exact zero-temperature spin coherence $\langle \sigma_x \rangle$ is controlled at large dissipation by the bare scale Δ / ω_c , which is much larger than the renormalized dimensionless tunneling energy Δ_R / ω_c predicted by single-polaron theory. This effect was shown in the main manuscript to arise from entanglement within the bath in the form of antipolaron contributions to the many body state.

We consider here the effect of finite temperature on the coherence, and demonstrate that, within a single-polaron approach, the coherence is strongly suppressed when the temperature reaches the scale Δ_R , while it is preserved up to much higher temperatures (of the order of the bare Δ) in the exact solution of the spin-boson model. This indicates that antipolaron-type entanglement persists within the low-lying thermal excitations. We suppose here that an external thermal bath couples to our spin-boson system such that the system thermalizes with respect to many-body states of the total spin-boson Hamiltonian.

Generalizing the many-polaron Ansatz to capture the free energy of the spin-boson model is a formidable task beyond the scope of the present analysis. In addition, we would like to have quantitative results for $\langle \sigma_x \rangle$ at finite

temperature that are independent of the coherent state expansion. We thus consider the solution of the spin-boson model at the exactly-solvable Toulouse line, namely for the dissipation strength $\alpha = 0.5$. In this case, the spin-boson model can be mapped onto a model of non-interacting electrons with a resonant level [1, 2]. The free energy can then be computed from the standard expression:

$$F = -T \int_{-D}^D d\epsilon \log [1 + e^{-\epsilon/T}] \rho(\epsilon), \quad (\text{S20})$$

with $\rho(\epsilon) = (T_K/\pi)/[\epsilon^2 + T_K^2]$ the effective electronic density of states of the equivalent resonant level model. Here, $D = 4\omega_c/\pi$ denotes the corresponding fermionic bandwidth and $T_K = \Delta^2/\omega_c$ is the Kondo scale. The spin coherence is readily obtained from the derivative of this free energy with respect to the tunneling amplitude:

$$\langle \sigma_x \rangle = -2 \frac{dF}{d\Delta} = \frac{4\Delta}{\pi D} T \int_{-D}^D d\epsilon \log [1 + e^{-\epsilon/T}] \frac{\epsilon^2 - T_K^2}{(\epsilon^2 + T_K^2)^2}. \quad (\text{S21})$$

This expression is numerically evaluated and shown as solid lines in Fig. S1 for two values of Δ .

We now compare these exact results to the one-polaron theory, which can be extended to finite temperature, [7] and provides a simple formula for the spin coherence:

$$\langle \sigma_x \rangle_{\text{1pol.}} = \frac{\Delta_R}{\Delta} \tanh \left(\frac{\Delta_R}{2T} \right). \quad (\text{S22})$$

Thus, the coherence is rapidly suppressed by thermal effects in the case of the single-polaron approximation when reaching a temperature that is of the order of the small scale $\Delta_R \propto T_K$, see the dashed curves in Fig. S1. Note in particular how the exact solutions develop long tails at high temperature, rather than the sharp decay found in the single-polaron theory, a hallmark of many-body Kondo-type problems and antipolaron contributions in the present spin-boson context. This comparison proves the relevance of antipolaron physics in the thermal excitations of the spin-boson model.

-
- [1] Leggett, A. J., Chakravarty, S., Dorsey, A. T., Fisher, M. P. A., Garg, A. & Zwerger W. Dynamics of the dissipative two-state system. *Rev. Mod. Phys.* **59**, 1 (1987).
 - [2] Weiss, U. *Quantum Dissipative Systems* (World Scientific, 1993).
 - [3] Silbey, R. & Harris, R. Variational calculation of the dynamics of a two level system interacting with a bath. *J. Chem. Phys.* **80**, 2615 (1984).

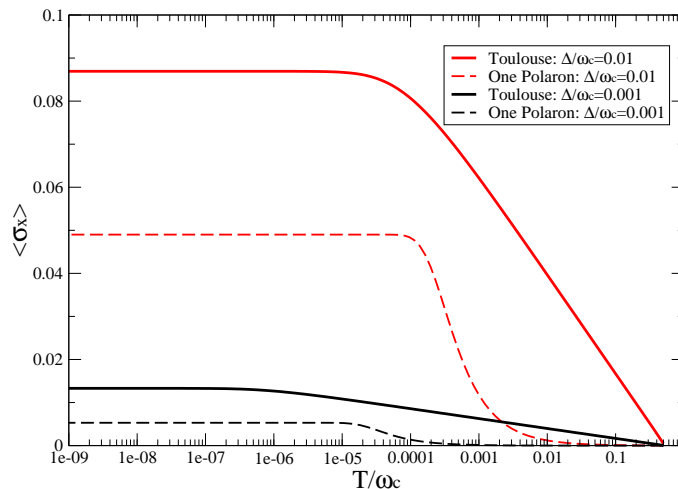


FIG. S1. Spin coherence at intermediate dissipation $\alpha = 0.5$ as a function of temperature for $\Delta/\omega_c = 0.001$ (black curves) and $\Delta/\omega_c = 0.01$ (red curves), computed from the exact Toulouse solution (solid lines) and from the one-polaron Silbey-Harris theory (dashed lines).

- [4] Raimond, J. M. & Haroche, S. *Understanding the Quantum* (Oxford Graduate Series, 2006).
- [5] Bulla, R., Costi, T. A. & Pruschke, T. Numerical renormalization group method for quantum impurity systems. *Rev. Mod. Phys.* **80**, 395 (2008).
- [6] Bulla, R., Tong, N.-H. & Vojta, M. Numerical renormalization group for bosonic systems and application to the sub-ohmic spin-boson model. *Phys. Rev. Lett.* **91**, 170601 (2003).
- [7] A. Nazir, D. P. S. McCutcheon, and A. W. Chin, *Phys. Rev. B* **85**, 224301 (2012).
- [8] K. Le Hur, *Ann. Phys.* **323**, 2208 (2008).
- [9] T. A. Costi and G. Zarand, *Phys. Rev. B* **59**, 12398 (1999).